

Loss of neuropilin1 inhibits liver cancer stem cells population and blocks metastasis in hepatocellular carcinoma via epithelial-mesenchymal transition

Xun LI^{1,2,*}, Yongqiang ZHOU³, JinJing HU^{2,4}, Zhongtian BAI¹, Wenbo MENG¹, Lei ZHANG¹, Xiaojing SONG¹, Yongjian WEI³, Jun YAN¹, Yihua ZHOU³

¹Department of General Surgery, The First Hospital of Lanzhou University; Cancer Prevention and Treatment Center of Lanzhou University School of Medicine, Lanzhou, China; ²Gansu Province Key Laboratory of Biotherapy and Regenerative Medicine, Lanzhou, China; ³The First Clinical Medical College of Lanzhou University, Lanzhou, China; ⁴School of Life Science of Lanzhou University, Lanzhou University, Lanzhou, China

*Correspondence: lxdr21@126.com

Received September 9, 2020 / Accepted November 20, 2020

It is generally believed that the existence of cancer stem cells (CSCs) is related to tumor recurrence and metastasis of hepatocellular carcinoma (HCC). Neuropilin1 (NRP1) is involved in numerous pathophysiological processes of tumor progression, however, whether NRP1 is involved in the regulation of liver CSCs and metastasis of HCC is still unknown. In the present study, we examined the effect of NRP1 on the population of liver CSCs and the metastasis mechanism of HCC. In NRP1 small hairpin RNA (shRNA)-transduced HCC cells, liver CSCs surface markers (CD133+/ EpCAM+/CD13+/CD44+) expressing cells, which imply the CSCs population, were decreased. Transwell assay and nude mouse liver orthotopic transplantation model confirmed that NRP1 knockdown inhibited HCC cells' migration and lung metastasis. Our data showed that the expression of NRP1 was upregulated in 5 independent cohorts of HCC patients, consequently, high levels of NRP1 correlated with recurrence and poor prognosis in HCC. Mechanism research showed that NRP1 promotes cell spreading through the epithelial-mesenchymal transition (EMT) signaling pathway. In summary, NRP1 enhanced the population of liver CSCs and migration of HCC via EMT, indicating that NRP1 might be a novel target for HCC treatments.

Key words: neuropilin1, hepatocellular carcinoma, liver cancer stem cells, tumor metastasis, epithelial-mesenchymal transition

Hepatocellular carcinoma (HCC) is one of the most common primary malignant tumors, causing a huge global health burden. Systematic and reasonable methods of screening, diagnosis, treatment, and follow-up have been formulated. However, morbidity and cancer-specific mortality have not been effectively controlled due to the lack of symptoms in the early stage, hidden onset, primary tumor heterogeneity, and tumor relapse [1].

The infinite differentiation potential and self-renewal properties of cancer stem cells (CSCs) are generally considered to be the causes of HCC cell growth, tumor heterogeneity, resistance to anti-cancer therapies, distant metastasis, recurrence, and treatment failure [2]. The identification of surface molecular targets expressed by CSCs and the investigation of regulatory mechanisms of targeting CSCs biological characteristics are critical to improving response to HCC therapeutic intervention [3]. A variety of markers for identification and isolation of liver cancer stem cells (LCSCs) have been reported, the representative markers are CD13, CD133, CD44, and epithelial cell adhesion molecule (EpCAM) [4].

The expression level of these CSCs surface markers can predict the potential of LCSCs to migrate, self-renew, and differentiate. The prospects for CSCs-targeting therapies are encouraging and optimistic [5], the researches of CSCs regulatory network are particularly important.

Neuropilin1 (NRP1), widely expressing in tumor vasculature, promotes angiogenesis and tumor progression by selectively binding to multiple extracellular signaling ligands [6]. NRP1 is involved in a wide range of pathophysiological processes, its expression and function in nerve cells, tumor cells, and immune cells have been extensively investigated [7]. In gastric cancer [8], breast cancer [9], colorectal cancer [10], oral squamous cell carcinoma [11], and lung cancer [12], elevated NRP1 expression is associated with cancer progression and poor clinical prognosis. NRP1 may be a promising target for cancer immunotherapy. CD8⁺ T cell-restricted NRP1-deficient mice are significantly more sensitive to PD1 immunotherapy [13]. The high proportion of NRP1^{-/-} regulatory T cells (Tregs) in the tumor enhances anti-tumor immunity and promotes tumor clearance [14]. During CSCs

promotes tumor progression and deterioration, angiogenesis is crucial, NRP1 acts as a vascular endothelial growth factor (VEGF) receptor, the regulation of NRP1 on CSCs has been attracting people's attention.

In the current study, we investigated the effect of NRP1 on the level of CD13, CD133, CD44, and EpCAM. The application of HCC cell lines, HCC tumor specimens, and liver orthotopic transplantation models verified that elevated NRP1 boosts migration, recurrence, and metastasis. The clinical prognosis of HCC patients with high expression of NRP1 is poor. Finally, we concluded that the high level of NRP1 elevates the proportion of LCSCs, thus promoting the malignant potential of HCC, and NRP1 may be used as a target for anti-LCSCs therapies.

Patients and methods

Patients and follow-up. Five independent patient cohorts were recruited as participants, with a total of 372 HCC patients (the cohorts, number of cases, sample source, and detection methods are summarized in Supplementary Table S1). Tumor and matched paracancer tissue were obtained after curative hepatic resections, which were performed at the Zhongshan Hospital of Fudan University during 2001–2010 and all patients gave written informed consent before the study. All cancers were verified histologically. The study was approved by the Hospital Ethics Committee and informed consent was obtained from each patient under Institutional Reviewer Board protocols. The study protocol conforms to the ethical guidelines of the 1975 Declaration of Helsinki as reflected in a priori approval by the institution's human research committee.

Tissue microarrays and immunohistochemistry. Paraffin-embedded tissue samples were obtained from 239 patients. Core samples from representative areas of each tumor were selected for H&E staining. Immunostaining of NRP1 was performed. Briefly, 4 μm tissue sections were deparaffinized and treated for antigen retrieval (citrate buffer, pH 6.0). Sections were then incubated (30 min) with rabbit monoclonal antibodies to NRP1 (1:100; Abcam), exposed to 3,3'-diaminobenzidine tetrahydrochloride, and counterstained with hematoxylin. Semi-quantitation was based on the intensity of staining of positive cells as follows: 0) <5%; 1) 6–35%; 2) 36–70%; 3) >70%. Slides were assessed by two observers independently.

RNA isolation and qRT-PCR. Total RNA was extracted using TRIzol reagent (Invitrogen, USA) as instructed by the manufacturer. NRP1 expression was analyzed using an ABI7900HT unit (Applied Biosystems, Foster City, USA). All qRT-PCR testing relied on TB Green Premix Ex Taq II (Takara Bio, Shiga, Japan), following the manufacturer's instructions. The primers are shown in Supplementary Table S2. Results were normalized using the endogenous control gene (GAPDH) expression. The relative expression levels of NRP1 were analyzed by the $2^{-\Delta\Delta\text{CT}}$ method. All experiments were done in triplicate.

Protein extraction and western blot analysis. Total protein extracted in RIPA (Beyotime, China) buffer containing 1% PMSF and phosphatase inhibitor from each subset, separated by SDS-PAGE and transferred to PVDF membranes. The membranes were blocked with skimmed milk and incubated (overnight, 4°C) with an anti-NRP1 monoclonal antibody (1:1000, Abcam). After washings with TBS-T, membranes were incubated (room temperature, 1 h) with horseradish peroxidase-conjugated secondary antibody and exposed to enhanced chemiluminescence reagent. To confirm equal protein loading, an anti- β -actin antibody (1:2000, Sigma, USA) was used to re-probe.

Cell culture and transfection. Huh7 and HCCLM3 cells purchased from the Chinese Academy of Sciences (Shanghai, China), all cells have STR profile report. Cells were grown in Dulbecco's modified Eagle's medium (DMEM, Gibco), 10% (v/v) fetal bovine serum (Hyclone, USA). Cells were cultured in a humidified incubator (Thermo Fisher Scientific, USA) at 37°C and 5% CO₂. NRP1 small hairpin RNA (NRP1 shRNA) and negative control lentivirus (NRP1 shRNA NC) were produced by GeneChem (Shanghai, China) and transfected according to the manufacturer's instructions. Stably transfected cells were used for subsequent experiments.

Transwell assays, colony formation assays, and sphere formation assays. After trypsinization (0.25% trypsin-EDTA, BI), the cell concentration was adjusted to 2×10^5 cells/ml. 600 μl of complete medium containing 30% (v/v) serum was added to the lower chamber and 200 μl of cell suspension was added to the upper chamber, and cultured for 48 h for transwell assays.

Cells were seeded in 6-well plates (Corning, USA) for colony formation assays. After 2 weeks of culture, cells were fixed with 4% paraformaldehyde (Solarbio, China), stained with 0.5% crystal violet (Solarbio, China), observed and photographed. Image pro plus 6.0 was used to count the number of cells.

2000 cells/well were planted on ultra-low attachment surface 6-well plates (Corning, USA). After 8 days of culture, cells were counted and the images were taken (random 15 fields/well) under a stereomicroscope (Olympus, Japan). Image pro plus 6.0 was performed to measure the diameter of the spheres, diameter >20 μm was considered as formed spheres.

In vivo experiment. Four-week-old nude mice were purchased from Beijing Vitalstar Biotechnology Co, Ltd (Beijing, China) and maintained in strict pathogen-free conditions at the Animal Center housed by Gansu University of Traditional Chinese Medicine. The liver orthotopic transplantation model was produced, according to standard procedures previously described [15]. The mice were sacrificed after 6 weeks. The liver, lung, and tumor tissues were taken out, fixed with 4% formalin, and embedded in paraffin. All animals received appropriate care and all procedures followed guidelines established by the National Institutes of Health Guide for the Care and Use of Laboratory Animals.

Flow cytometry and cell analysis. Phycoerythrin (PE)-conjugated CD133 antibody (cat. no. 130-110-962), PE-Vio770-conjugated CD13 antibody (cat. no. 130-120-727), allophycocyanin (APC)-conjugated EpCAM antibody (cat. no. 130-111-000), APC-Vio770-conjugated CD44 antibody (cat. no. 130-113-339), and isotype control antibody (cat. no. 130-113-438, 130-113-440, 130-113-434, 130-113-435, respectively) were all purchased from Miltenyi Biotec (Bergisch Gladbach, Germany). The corresponding antibody was used according to the manufacturer's instructions. The percentage of CD133, CD13, EpCAM, and CD44 in the cell population was detected using BD LSRFortessa. All experiments were done in triplicate.

Bioinformatics analysis. Related genes of NRP1 were selected from the Cbioportal (<https://www.cbioportal.org/>), Coexpedia (<http://www.coexpedia.org/>), Ualcan (<http://ualcan.path.uab.edu/>), and Genecards (<https://www.genecards.org/>) database, 123 intersection genes were screened out. FunRich 3.1.3 (<http://www.funrich.org/>) software was used for GO analysis and KEGG pathway analysis of NRP1 related genes.

Statistical analysis. Standard software (SPSS 24.0 for Windows; SPSS Inc., Chicago, IL, USA) was used for all statistical analyses and $p < 0.05$ was considered statistically significant. A Student's t-test or one-way ANOVA were used for comparisons of quantitative data of groups. Categorical data were subjected to chi-square testing. Overall survival (OS) and cumulative recurrence rates were estimated by the Kaplan-Meier method, and differences were determined using a log-rank test. Univariate and multivariate analyses were performed using Cox proportional hazards regression model.

Results

NRP1 drives the stem-like properties of HCC. To evaluate the regulation of NRP1 in liver cancer stem cells, small hairpin RNA (shRNA) was used to transfect HCCLM3 and Huh7 cells. To confirm that NRP1 shRNA suppressed the expression of NRP1, qRT-PCR and western blot were used to confirm the expression level of NRP1 mRNA and NRP1 protein. Our results showed that the expression of NRP1 mRNA and NRP1 protein decreased significantly after transfection of NRP1 shRNA (Figures 2A–2B). The cells expressing the surface markers (CD13/CD133/EpCAM/CD44) of liver CSCs were detected by flow cytometry to investigate the effect of NRP1 on the CSCs population.

In HCCLM3 cells, the percentage of CD133⁺, EpCAM⁺, CD13⁺, CD44⁺ was significantly reduced in NRP1-sh1 transfected cells. The percentage of CD13⁺ and EpCAM⁺ was decreased by stably transfected NRP1-sh2 (Figure 1A).

The same experiment was performed in Huh7 cells to confirm the regulatory effect of NRP1 on liver CSCs. The decreased proportion of CD133⁺, EpCAM⁺, CD13⁺, CD44⁺ was also observed after NRP1-sh1 transfection in Huh7 cells,

the proportion of CD133⁺, CD13⁺ was reduced by transfection with NRP1-sh2 (Figure 1B). In summary, these data indicate that in human HCC, NRP1 negatively regulates the populations of CSCs.

To investigate whether NRP1 knockdown affects the proliferation and self-renewal ability of HCC cells, we conducted the colony formation assay. In the colony formation analysis of HCCLM3 and Huh7 cell lines, a lack of proliferation and self-renewal was observed after NRP1 knockdown (Figures 1C, 1D). Sphere formation assays were performed to further validate the influence of NRP1 on the stem-like properties of HCC, the diameter of the spheres were significantly smaller when transfected with NRP1 shRNA compared with the negative control lentivirus transfection (Figures 1E, 1F). These results provide common evidence that NRP1 is essential for driving the properties of cells with stem cell characteristics in HCC.

Decreased NRP1 levels negatively correlated with metastasis of HCC cell lines. As the knockdown of NRP1 inhibits the expression of CSCs surface markers, we speculated that NRP1 is related to the migration and metastasis of HCC. First, we detected the expression level of NRP1 mRNA and NRP1 protein in human L02 hepatocytes and several liver cancer cell lines (HepG2, Huh7, HCCLM3) by qRT-PCR and western blot. The level of NRP1 mRNA and NRP1 protein in HCC cell lines was higher compared to L02 cells (Supplementary Figure S1A). To validate the effects of NRP1 on the migration capacity of HCC cells, HCCLM3 and Huh7 cells were transfected with NRP1 knockdown or negative control lentivirus. The transwell assays confirmed that the number of migrated cells of NRP1 shRNA transfected cells was significantly lower than negative control transfected cells (Figures 2C, 2D).

To investigate whether NRP1 knockdown also affects tumor formation and lung metastasis potential *in vivo*, HCCLM3 cells were transfected with NRP1 knockdown or negative control lentivirus, then the transfected cells were transplanted into the liver of nude mice *in situ*. After transplantation of the HCC cells into nude mice, all subsets succeeded in forming subcutaneous tumors (Supplementary Figure S1B). In the liver orthotopic transplantation model, pulmonary metastasis occurred in 100% (5/5) of the HCCLM3-NC grafted mice, which was higher than the rate observed in the HCCLM3-shNRP1 (1/5) grafts. The number of each grade of metastatic nodules stemming from the HCCLM3-NC grafts was also greater (Figure 2E). Thus, our findings suggested that high NRP1 expression could be related to the migration and metastasis of HCC.

NRP1 upregulation is indicative of poor prognosis and recurrence. We found that NRP1 promotes HCC metastasis is confirmed by *in vivo* and *in vitro* experiments. However, the clinical and prognostic characteristics of NRP1 in HCC patients still unknown. To address this issue, qRT-PCR analysis of tissue from 81 HCC patients (cohort 1, n=81) revealed elevated expression of NRP1 in 64% of the tumor

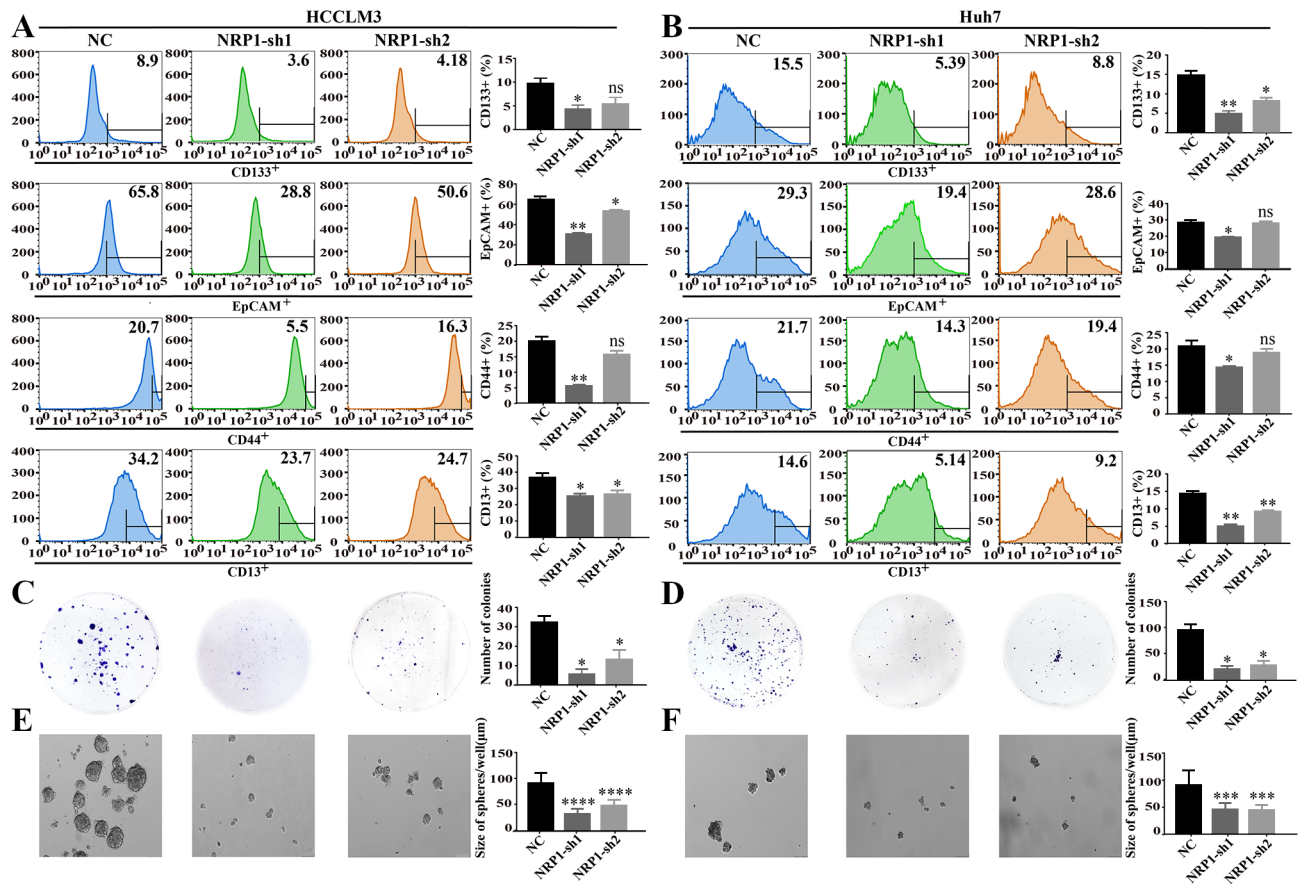


Figure 1. NRP1 drives the stem-like properties of HCC. A–B) NRP1 small hairpin RNA and negative control lentivirus transfected HCCLM3 and Huh7 cells for 72 h. Flow cytometry results showing the percentage of CD133⁺, EpCAM⁺, CD44⁺, CD13⁺ in stably transfected cells. The ordinate represents the cell number, the abscissa indicates the fluorescence intensity. Three independent repeated tests showing with histogram. C–D). Colony formation of stably transfected HCCLM3 and Huh7 cells. Counting the number of cells with image-Pro plus 6.0. E–F) Image shows the sphere formation stably transfected HCCLM3 and Huh7 cells, histogram shows the diameter of the spheres in each well. One-way ANOVA was used to show a statistical difference. Results are shown as means ± SD. **p*<0.05, ***p*<0.01, ****p*<0.001, *****p*<0.0001, ns means no significance.

tissue samples compared to 36% of paracancer tissue samples (Figure 3A). Western blot detected NRP1 expression in tumor tissues and paracancer tissue of 16 randomly selected HCC patients (cohort 2, *n*=16), the increased expression of NRP1 can be detected in 62.5% (10/16) of tumor tissues compared to 37.5% (6/16) of paracancer tissue (Figure 3B). NRP1 expression was scored by immunohistochemical staining in HCC samples from 239 patients (cohort 3, *n*=239). Semi-quantitative analysis of NRP1 expression was performed based on the density of cells staining as follows: 0) <5%; 1) 6–35%; 2) 36–70%; 3) >70% (the scoring standard of NRP1 expression is shown in Supplementary Figure S1C). Specimens with scores of 0 and 1 are regarded as low expression of NRP1 (NRP1_{Low}), while specimens with scores of 2 and 3 are classified as high expression of NRP1 (NRP1_{High}). The OS (overall survival) between the NRP1_{High} group and the NRP1_{Low} group were analyzed.

As of the date of the last follow-up (March 2009), 57.3% (137/239) of the patients had died. In this cohort, OS of

the NRP1_{High} group was significantly lower than that of the NRP1_{Low} group (log Rank=24.953; *p*=0.000) (Figure 3C).

36 HCC tumors sampled from randomly recruited patients (cohort 4, *n*=16; cohort 5, *n*=20), 18 suffered recurrences and the remaining were recurrence-free at 2 years. Western blot and qRT-PCR were used to detect the expression of NRP1 in HCC patients with and without recurrence. The results showed that the expression level of NRP1 in patients with recurrence was higher than that in patients without recurrence (Figures 3D, 3E).

The expression of NRP1 is an independent prognostic factor affecting OS. We analyzed the clinical data of 239 HCC patients whose samples underwent immunohistochemical staining. Clinical parameters collected included gender, age, AFP levels, Child-Pugh scores, tumor sizes, tumor microvascular invasion, pathological stages, and so on.

Table 1 shows the correlation analysis results between the expression of NRP1 and clinicopathological characteristics. It can be seen that the expression of NRP1 is correlated with

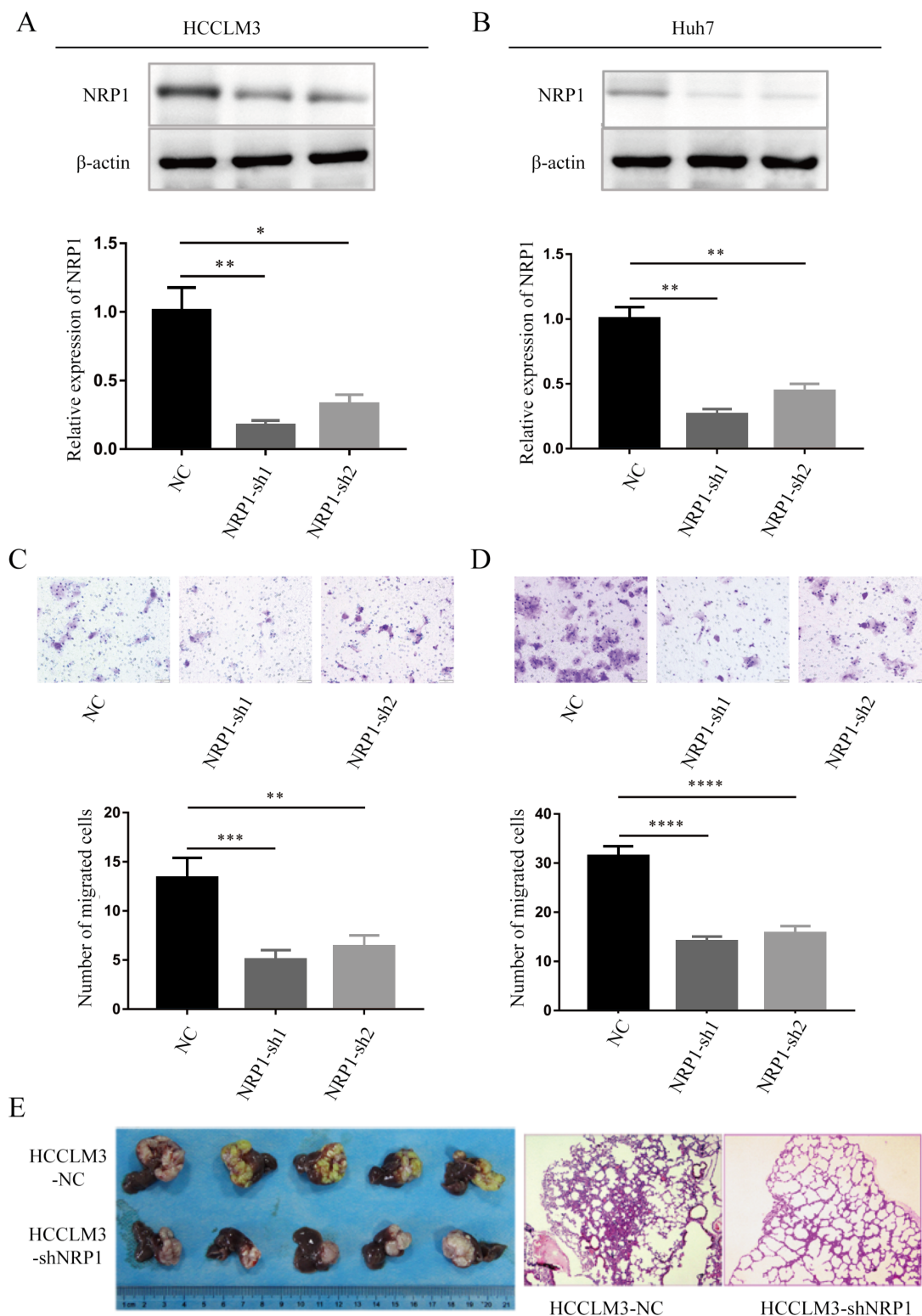


Figure 2. Decreased NRP1 levels negatively correlated with metastasis of HCC cell lines. A–B) Western blot and real-time quantitative PCR were used to detect the expression of NRP1 mRNA and NRP1 protein in HCCLM3 and Huh7 cells to verify the knockdown effect. C–D) The effect of NRP1 knockdown on the migration of HCCLM3 and Huh7 cells was evaluated by transwell assays. E) Liver orthotopic transplantation model was produced through transfection of HCCLM3-NC and HCCLM3-shNRP1 cells. Lung metastatic nodules were observed. One-way ANOVA was used to show a statistical difference. Results are shown as means \pm SD. * $p < 0.05$, ** $p < 0.01$, *** $p < 0.001$, **** $p < 0.0001$.

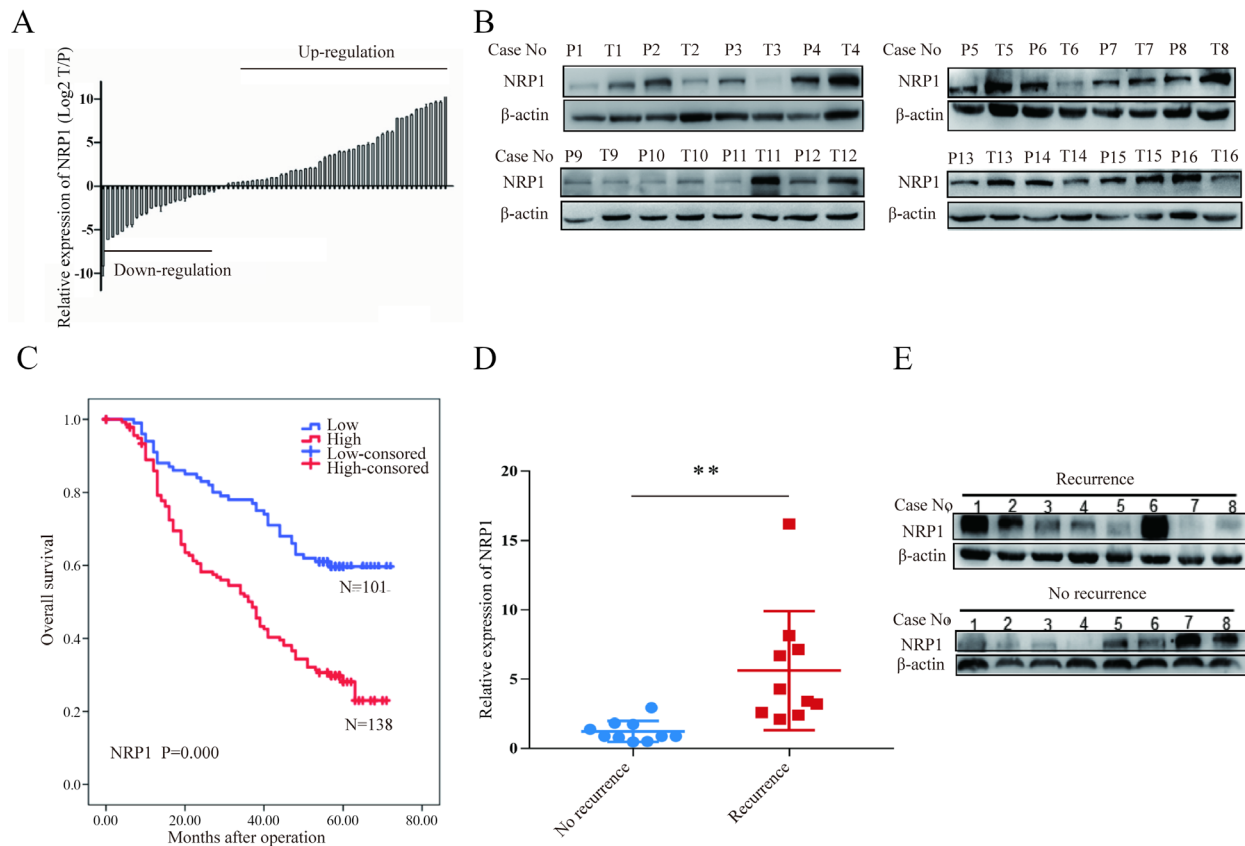


Figure 3. NRP1 upregulation is indicative of poor prognosis and recurrence. A) The expression of NRP1 was detected by qRT-PCR in 81 cases of the tumor and adjacent tissues (cohort 1). B) Western blot showed the expression of NRP1 in 16 cases of the tumor and adjacent tissues (cohort 2). C) Kaplan-Meier analysis between OS and 239 HCC patients with high or low expression of NRP1 (cohort 3). D) The expression of NRP1 was detected by qRT-PCR in 10 recurrence and 10 non-recurrence HCC patients (cohort 4), t-test, $**p < 0.01$. E) Western blot showed the expression of NRP1 in 8 recurrence and 8 non-recurrence patients (cohort 5). T means tumor tissue, P means paracancer tissue.

the presence or absence of vascular invasion ($p = 0.007$), but has no correlation with other clinical indicators.

Using COX regression analysis, the univariate analysis showed that the risk factors affecting liver cancer OS were portal vein tumor thrombus (1.590 (1.007–2.510), $p = 0.047$) and the expression of NRP1 (2.465 (1.703–3.570), $p = 0.000$) (Table 2).

Multivariate analysis of the single-factor risk factors showed that the expression of NRP1 (2.292 (1.578–3.329), $p = 0.000$) is an independent prognostic factor that affects OS (Table 2).

NRP1 functions by regulating the EMT signaling pathway *in vitro*. To further evaluate the mechanism of NRP1 in promoting HCC metastasis, recurrence, and poor prognosis bioinformatics methods were used to screen out 123 NRP1 related genes (Supplementary Table S1) from four databases (Figure 4A). KEGG enrichment analysis of related genes revealed that NRP1 mainly functions through the EMT signaling pathway (Figure 4B). Western blot analysis showed that knockdown of NRP1 restored E-cadherin expression and reduced N-cadherin and Vimentin expres-

sion in HCCLM3 and Huh7 cells (Figure 4C). Verified that NRP1 promotes HCC cells' metastasis by regulating the EMT signaling pathway.

Discussion

A lot of convincing evidence has revealed that the existence of cancer stem cells (CSCs) is responsible for HCC metastasis, recurrence, and heterogeneity [16]. Here, we identified that the knockdown of NRP1 suppresses the population of CSCs representative surface markers (CD133⁺/EpCAM⁺/CD13⁺), inhibits the migration of HCC cells, and the recurrence and prognosis of HCC patients.

It has been recently demonstrated that NRP1 has tumor-inducing properties [17], promotes survival of CSCs [18], enhances resistance to chemotherapy drugs [11], the VEGF-Nrp1 axis regulates tumor initiation and stemness [19], and promotes the viability of glioma stem-like cells and tumor growth [20], NRP1 may be a useful biomarker for tumor-initiating cells or CSCs. Our research focuses on the effect of NRP1 on liver CSCs and shows the expression of

Table 1. Correlation between the factors and clinicopathological characteristics in HCC (n=239).

Clinicopathological indexes	NRP1		p-value
	Low	High	
HBV			
Negative	68 (63.7%)	96 (69.6%)	0.713
Positive	33 (32.7%)	42 (30.4%)	
Portal vein tumor thrombus			
No	90 (89.1%)	117 (84.8%)	0.332
Yes	11 (10.9%)	21 (15.2%)	
Extrahepatic bile duct/gallbladder invasion			
No	95 (94.1%)	133 (96.4%)	0.398
Yes	6 (5.9%)	5 (3.6%)	
Gender			
Male	91 (90.1%)	124 (89.9%)	0.951
Female	10 (9.9%)	14 (10.1%)	
Age (year)			
≤50	31 (30.7%)	59 (42.8%)	0.057
>50	70 (69.3%)	79 (57.2%)	
Vascular invasion			
No	61 (60.4%)	59 (42.8%)	0.007
Yes	40 (39.6%)	79 (57.2%)	
Tumor number			
Single	92 (91.1%)	122 (88.4%)	0.503
Multiple	9 (8.9%)	16 (11.6%)	
Metastasis			
No	95 (94.1%)	127 (92.0%)	0.546
Yes	6 (5.9%)	11 (8.0%)	
Liver cirrhosis			
No	61 (60.4%)	89 (64.5%)	0.518
Yes	40 (39.6%)	49 (35.5%)	
Tumor size (cm)			
≤5	45(44.6%)	50 (36.2%)	0.194
>5	56 (55.4%)	88 (63.8%)	
Pathological stages			
I/II	18 (17.8%)	20 (14.5%)	0.487
III/IV	83 (82.2%)	118 (85.5%)	
AFP (ng/ml)			
≤20	16 (15.8%)	28 (20.3%)	0.381
>20	85 (84.2%)	110 (79.7%)	

Table 2. Univariate and multivariate analyses of prognostic factors in HCC (n=239).

Variable	OS	
	HR (95% CI)	p-value
Univariate analysis		
HBV	1.280 (0.901–1.819)	0.168
Portal vein tumor thrombus	1.590 (1.007–2.510)	0.047
Extrahepatic bile duct/gallbladder invasion	1.597 (0.746–3.421)	0.228
Gender (female vs. male)	0.726 (0.401–1.313)	0.289
Age, year (≤50 vs. >50)	1.003 (0.717–1.402)	0.988
Vascular invasion	1.219 (0.871–1.701)	0.249
Tumor number (single vs. multiple)	1.610 (0.979–2.646)	0.060
Metastasis	1.259 (0.696–2.278)	0.446
Liver cirrhosis	0.946 (0.667–1.342)	0.755
Tumor size, cm (≤5 vs. >5)	1.089 (0.774–1.533)	0.623
Pathological stages (I/II vs. III/ IV)	1.030 (0.652–1.626)	0.900
AFP, ng/ml (≤20 vs. >20)	1.254 (0.801–1.963)	0.322
NRP1 (low vs. high)	2.465 (1.703–3.570)	<0.001
Multivariate analysis		
Portal vein tumor thrombus	1.517 (0.957–2.403)	0.076
NRP1 (low vs. high)	2.292 (1.578–3.329)	<0.001

CSCs surface markers and self-renewal observed through colony formation are decreased after NRP1 knockdown. CD133 and EpCAM are the most important markers of liver CSCs [21]. Our results showed that after knocking down NRP1, the expression of CD133 and EPCAM decreased significantly, thus proving the important role of NRP1 in liver CSCs, which consistent with the research of Liu et al. [22]. They proposed that miR-148b plays key role in maintaining the CSCs characteristics of side population cells by targeting NRP1. OCT4, SOX2, and NANOG constitute the core transcription factors that regulate stem cell self-renewal, and are commonly used to characterize CSCs, but they are mainly distributed in

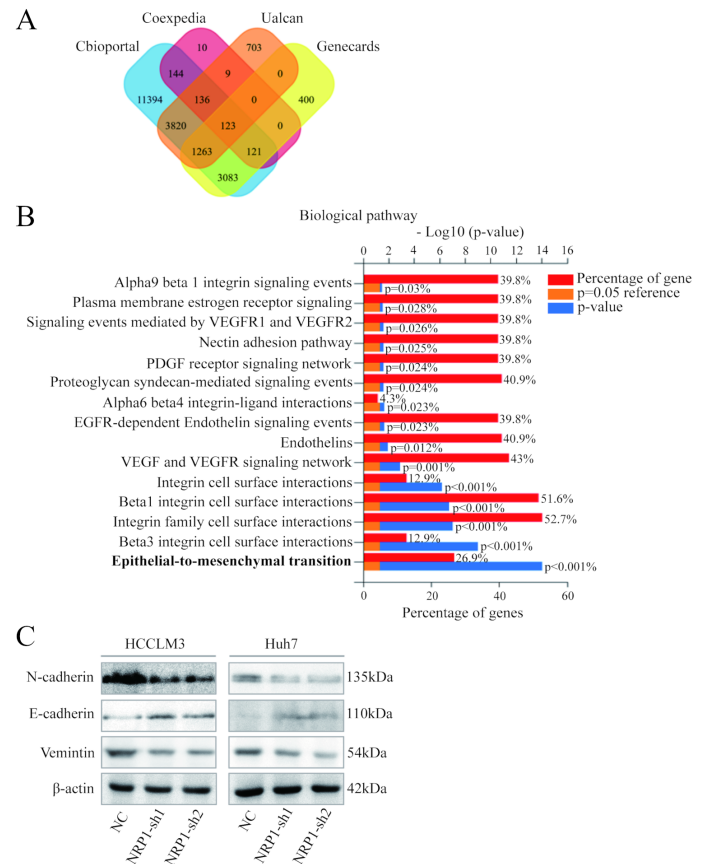


Figure 4. NRP1 functions by regulating the EMT signaling pathway *in vitro*. A) Related genes of NRP1 were chosen in hepatocellular carcinoma (HCC) from the Cbioportal, Coexpedia, Ualcan, and Genecards, 123 intersection genes were screened out. B) KEGG enrichment analysis of NRP1 related genes by Funrich. C) Expression of E-cadherin, N-cadherin, and Vimentin in HCCLM3 and Huh7 cells with NRP1 knockdown and negative control were detected by western blot. β-Actin was used as a loading control.

the nucleus and are not easily detected [23]. The development of membrane surface markers such as NRP1 for CSCs characterization is crucial. NRP1 may be used as a new CSCs surface marker, which is a very interesting aspect worth studying.

Knockdown or overexpression of different stemness-related genes of CSCs to construct super-stem maintenance CSCs (super-CSCs). After establishing this super-CSCs model, we will investigate the characteristics of CSCs more deeply and effectively. Our laboratory has made some efforts in this aspect. NRP1 is one of the preliminary attempts to construct a super-CSCs model. The identification and sorting of new CSCs markers based on the super-CSCs model may be a promising prospect and direction for future CSCs researches.

Accumulating evidence shows that NRP1 is a tumor-promoting factor, upregulated in a variety of tumors, promoting proliferation and metastasis [24]. From the perspective of NRP1 promoting the proportion of surface markers of liver CSCs, our research inferred that NRP1 is related to the clinical features of HCC. Through qRT-PCR, western blot, and immunohistochemistry we observed that NRP1 is highly expressed in HCC and an elevated level of NRP1 promotes HCC recurrence and poor prognosis. The study of Lin et al. [25] showed that serum NRP1 has better diagnostic performance for HCC than AFP, and knocking down NRP1 inhibits the phenotype of HCC cells. Lin's and our research together suggest that NRP1 can be used as a diagnostic and potential prognostic target for HCC.

In summary, our study provides a better understanding of the molecular mechanisms of NRP1 involved in HCC metastasis. Furthermore, our results suggest a potential role of NRP1 as a biomarker of disease progression and prognosis in HCC patients.

Supplementary information is available in the online version of the paper.

Acknowledgments: This work was supported by the Science and Technology Major Project of Gansu province (1602FKDA001), the Talent innovation and Entrepreneurship Program of Lanzhou City (2016-RC-57), Gansu Province Science and Technology Plan Project Mission Statement (18JR2TA018), the Science and Technology Project of Chengguan District (2017SHFZ0014) and Gansu Province Health Industry Scientific Research Project (GWSKY-2015-490).

References

- [1] SINGAI A, LAMPERTICO P, NAHON P. Epidemiology and surveillance for hepatocellular carcinoma: New trends. *J Hepatol* 2020; 72: 250–261. <https://doi.org/10.1016/j.jhep.2019.08.025>
- [2] DATTILO R, MOTTINI C, CAMERA E, LAMOLINARA A, AUSLANDER N et al. Pyrvinium pamoate induces death of triple-negative breast cancer stem-like cells and reduces metastases through effects on lipid anabolism. *Cancer Res* 2020. <https://doi.org/10.1158/0008-5472.CAN-19-1184>
- [3] GARCIA-MAYEA Y, MIR C, MASSON F, PACIUCCI R, ME LL. Insights into new mechanisms and models of cancer stem cell multidrug resistance. *Semin Cancer Biol* 2020; 60: 166–180. <https://doi.org/10.1016/j.semcancer.2019.07.022>
- [4] WU J, ZHU P, LU T, DU Y, WANG Y et al. The long non-coding RNA LncHDAC2 drives the self-renewal of liver cancer stem cells via activation of Hedgehog signaling. *J Hepatol* 2019; 70: 918–929. <https://doi.org/10.1016/j.jhep.2018.12.015>
- [5] COLE AJ, FAYOMI AP, ANYAECHE VI, BAI S, BUCKANOVICH RJ. An evolving paradigm of cancer stem cell hierarchies: therapeutic implications. *Theranostics* 2020; 10: 3083–3098. <https://doi.org/10.7150/thno.41647>
- [6] WEI Y, GUO S, TANG J, WEN J, WANG H et al. MicroRNA-19b-3p suppresses gastric cancer development by negatively regulating neuropilin-1. *Cancer Cell Int* 2020; 20: 193. <https://doi.org/10.1186/s12935-020-01257-0>
- [7] KO JH, KWON HS, KIM B, MIN G, SHIN C et al. Preclinical Efficacy and Safety of an Anti-Human VEGFA and Anti-Human NRP1 Dual-Targeting Bispecific Antibody (IDB0076). *Biomolecules* 2020; 10: 919. <https://doi.org/10.3390/biom10060919>
- [8] MEI B, CHEN J, YANG N, PENG Y. The regulatory mechanism and biological significance of the Snail-miR590-VEGFR-NRP1 axis in the angiogenesis, growth and metastasis of gastric cancer. *Cell Death Dis* 2020; 11: 241. <https://doi.org/10.1038/s41419-020-2428-x>
- [9] RIZZOLIO S, CAGNONI G, BATTISTINI C, BONELLI S, ISELLA C et al. Neuropilin-1 upregulation elicits adaptive resistance to oncogene-targeted therapies. *J Clin Invest* 2018; 128: 3976–3990. <https://doi.org/10.1172/JCI99257>
- [10] MA LL, GUO LL, LUO Y, LIU GL, LEI Y et al. Cdc42 subcellular relocation in response to VEGF/NRP1 engagement is associated with the poor prognosis of colorectal cancer. *Cell Death Dis* 2020; 11: 171. <https://doi.org/10.1038/s41419-020-2370-y>
- [11] CHU WM, SONG XM, YANG XM, MA L, ZHU J et al. Neuropilin-1 promotes epithelial-to-mesenchymal transition by stimulating nuclear factor-kappa B and is associated with poor prognosis in human oral squamous cell carcinoma. *PLoS One* 2014; 9: e101931. <https://doi.org/10.1371/journal.pone.0101931>
- [12] DING Z, DU W, LEI Z, ZHANG Y, ZHU J et al. Neuropilin 1 modulates TGFbeta1-induced epithelial-mesenchymal transition in nonsmall cell lung cancer. *Int J Oncol* 2020; 56: 531–543. <https://doi.org/10.3892/ijo.2019.4938>
- [13] LIU C, SOMASUNDARAM A, MANNE S, GOCHER AM, SZYMCAK-WORKMAN AL et al. Neuropilin-1 is a T cell memory checkpoint limiting long-term antitumor immunity. *Nat Immunol* 2020. <https://doi.org/10.1038/s41590-020-0733-2>
- [14] OVERACRE-DELGOFFE AE, CHIKINA M, DADEY RE, YANO H, BRUNAZZI EA et al. Interferon-gamma Drives Treg Fragility to Promote Anti-tumor Immunity. *Cell* 2017; 169: 1130–1141 e1111. <https://doi.org/10.1016/j.cell.2017.05.005>

- [15] LI CX, LING CC, SHAO Y, XU A, LI XC et al. CXCL10/CXCR3 signaling mobilized-regulatory T cells promote liver tumor recurrence after transplantation. *J Hepatol* 2016; 65: 944–952. <https://doi.org/10.1016/j.jhep.2016.05.032>
- [16] HUANG T, SONG X, XU D, TIEK D, GOENKA A et al. Stem cell programs in cancer initiation, progression, and therapy resistance. *Theranostics* 2020; 10: 8721–8743. <https://doi.org/10.7150/thno.41648>
- [17] JIMENEZ-HERNANDEZ LE, VAZQUEZ-SANTILLAN K, CASTRO- OROPEZA R, MARTINEZ-RUIZ G, MUNOZ-GALINDO L et al. NRP1-positive lung cancer cells possess tumor-initiating properties. *Oncol Rep* 2018; 39: 349–357. <https://doi.org/10.3892/or.2017.6089>
- [18] GRUN D, ADHIKARY G, ECKERT RL. NRP-1 interacts with GIPC1 and SYX to activate p38 MAPK signaling and cancer stem cell survival. *Molecular carcinogenesis* 2019; 58: 488–499. <https://doi.org/10.1002/mc.22943>
- [19] BECK B, DRIESSENS G, GOOSSENS S, YOUSSEF KK, KUCHNIO A et al. A vascular niche and a VEGF-Nrp1 loop regulate the initiation and stemness of skin tumours. *Nature* 2011; 478: 399–403. <https://doi.org/10.1038/nature10525>
- [20] HAMERLIK P, LATHIA JD, RASMUSSEN R, WU Q, BARTKOVA J et al. Autocrine VEGF-VEGFR2-Neuropilin-1 signaling promotes glioma stem-like cell viability and tumor growth. *The Journal of experimental medicine* 2012; 209: 507–520. <https://doi.org/10.1084/jem.20111424>
- [21] CASTELLI G, PELOSI E, TESTA U. Liver Cancer: Molecular Characterization, Clonal Evolution and Cancer Stem Cells. *Cancers (Basel)* 2017; 9. <https://doi.org/10.3390/cancers9090127>
- [22] LIU Q, XU Y, WEI S, GAO W, CHEN L et al. miRNA-148b suppresses hepatic cancer stem cell by targeting neuropilin-1. *Bioscience reports* 2015; 35. <https://doi.org/10.1042/bsr20150084>
- [23] KAUFHOLD S, GARBAN H, BONAVIDA B. Yin Yang 1 is associated with cancer stem cell transcription factors (SOX2, OCT4, BMI1) and clinical implication. *J Exp Clin Cancer Res* 2016; 35: 84. <https://doi.org/10.1186/s13046-016-0359-2>
- [24] DUMOND A, PAGES G. Neuropilins, as Relevant Oncology Target: Their Role in the Tumoral Microenvironment. *Front Cell Dev Biol* 2020; 8: 662. <https://doi.org/10.3389/fcell.2020.00662>
- [25] LIN J, ZHANG Y, WU J, LI L, CHEN N et al. Neuropilin 1 (NRP1) is a novel tumor marker in hepatocellular carcinoma. *Clin Chim Acta* 2018; 485: 158–165. <https://doi.org/10.1016/j.cca.2018.06.046>

https://doi.org/10.4149/neo_2020_200914N982

Loss of neuropilin1 inhibits liver cancer stem cells population and blocks metastasis in hepatocellular carcinoma via epithelial-mesenchymal transition

Xun LI^{1,2,*}, Yongqiang ZHOU³, JinJing HU^{2,4}, Zhongtian BAI¹, Wenbo MENG¹, Lei ZHANG¹, Xiaojing SONG¹, Yongjian WEI³, Jun YAN¹, Yihua ZHOU³

Supplementary Information

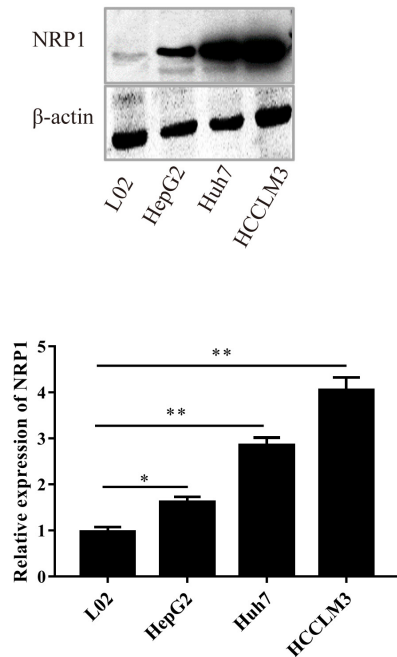
Supplementary Table S1. Information on NRP1 related genes.

Genes	Genes description	Biological functions in HCC	Genes	Genes description	Biological functions in HCC
NRP1	Neuropilin 1	Prognosis	CXCL12	C-X-C motif chemokine ligand 12	Metastasis
CD93	CD93 molecule	Prognosis	DPYSL2	dihydropyrimidinase like 2	No results
DAB2	DAB adaptor protein 2	Metastasis	PMP22	peripheral myelin protein 22	No results
TGFBR2	Transforming growth factor beta receptor 2	Invasion	WWTR1	WW domain containing transcription regulator 1	Prognosis
COL4A1	Collagen type IV alpha 1 chain	Metastasis	COL1A1	collagen type I alpha 1 chain	Invasion
VIM	Vimentin	Metastasis	GNB4	G protein subunit beta 4	No results
LAMB1	laminin subunit beta 1	No results	PLXND1	plexin D	No results
ZEB1	zinc finger E-box binding homeobox 1	Metastasis	CALCRL	calcitonin receptor like receptor	No results
NID2	nidogen 2	Prognosis	GNG12	G protein subunit gamma 12	No results
LAMA4	laminin subunit alpha 4	Metastasis	CRIM1	cysteine rich transmembrane BMP regulator 1	No results
COL6A2	collagen type VI alpha 2 chain	No results	RGS5	regulator of G protein signaling 5	Metastasis
VCAN	Versican	Metastasis	ATP2C1	ATPase secretory pathway Ca2+ transporting 1	No results
LAMC1	laminin subunit gamma 1	Prognosis	TCF7L2	transcription factor 7 like 2	Progression
COL4A2	collagen type IV alpha 2 chain	Prognosis	EDNRA	endothelin receptor type A	No results
PDGFRB	platelet derived growth factor receptor alpha	No results	SH2B3	SH2B adaptor protein 3	No results
CAV1	caveolin 1	Metastasis	FCGR2A	Fc fragment of IgG receptor IIa	No results
AXL	AXL receptor tyrosine kinase	Invasion	LYC3	lymphocyte cytosolic protein 2	No results
PDGFRB	platelet derived growth factor receptor beta	No results	SPP1	secreted phosphoprotein 1	Progression
COL6A3	collagen type VI alpha 3 chain	No results	ITGA6	integrin subunit alpha 6	No results
TCF4	transcription factor 4	Migration	TUBA1A	tubulin alpha 1a	No results
KCTD12	potassium channel tetramerization domain containing 12	No results	FPR3	formyl peptide receptor 3	No results
ANXA1	annexin A1	Prognosis	NOTCH2	notch receptor 2	Invasion
CD163	CD163 molecule	No results	RBBP7	RB binding protein 7, chromatin remodeling factor	No results
FSTL1	folliculin like 1	No results	PTGER4	prostaglandin E receptor 4	No results
IGFBP7	insulin like growth factor binding protein 7	No results	FBN1	fibrillin 1	No results
COL3A1	collagen type III alpha 1 chain	No results	PTPRB	protein tyrosine phosphatase receptor type B	Migration
MMRN2	multimerin 2	No results	LPAR6	lysophosphatidic acid receptor 6	No results
SPARC	secreted protein acidic and cysteine rich	Tumor growth	PLD1	phospholipase D1	Migration
MSN	Moesin	Metastasis	NCK2	NCK adaptor protein 2	No results
COL5A1	collagen type V alpha 1 chain	No results	SNRK	SNF related kinase	No results
HSPG2	heparan sulfate proteoglycan 2	No results	TUBB6	tubulin beta 6 class V	No results
FERMT2	fermitin family member 2	Metastasis	TNS3	tensin 3	No results
GJA1	gap junction protein alpha 1	No results	CTBP2	C-terminal binding protein 2	Invasion
CD44	CD44 molecule	Metastasis	PTPRM	protein tyrosine phosphatase receptor type M	No results
PRKD3	protein kinase D3	No results	PKP4	plakophilin 4	No results
CDH5	cadherin 5	No results	COL5A2	collagen type V alpha 2 chain	No results
ETS1	ETS proto-oncogene 1, transcription factor	Progression	ITGA3	integrin subunit alpha 3	Proliferation
PRKCH	protein kinase C eta	No results	ST8SIA4	ST8 alpha-N-acetyl-neuraminidase alpha-2,8-sialyltransferase 4	No results
TIMP2	TIMP metalloproteinase inhibitor 2	No results	SPRY1	sprouty RTK signaling antagonist 1	Prognosis
ARHGAP29	Rho GTPase activating protein 29	No results	GSN	Gelsolin	Prognosis
HEPH	Hephaestin	No results	NRIP1	nuclear receptor interacting protein 1	No results
MEF2C	myocyte enhancer factor 2C	Malignancy			

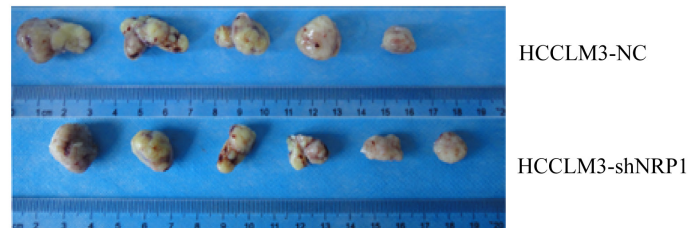
Supplementary Table S1. Continued ...

Genes	Genes description	Biological functions in HCC	Genes	Genes description	Biological functions in HCC
LTBP1	latent transforming growth factor beta binding protein 1	Proliferation	RPS6KA2	ribosomal protein S6 kinase A2	No results
COL12A1	collagen type XII alpha 1 chain	No results	EPS8	epidermal growth factor receptor pathway substrate 8	Metastasis
PRKCI	protein kinase C iota	No results	TIMP3	TIMP metalloproteinase inhibitor 3	Migration
AKT3	AKT serine/threonine kinase 3	Cell growth	SPRY2	sprouty RTK signaling antagonist 2	Progression
IPO5	importin 5	No results	LAMB2	laminin subunit beta 2	Metastasis
EMILIN1	elastin microfibril interfacier 1	No results	VDAC1	voltage dependent anion channel 1	Metastasis
TAF15	TATA-box binding protein associated factor 15	No results	ATP6V1D	ATPase H ⁺ transporting V1 subunit D	No results
CTNNA1	catenin alpha 1	Prognosis	MYO1E	myosin IE	No results
EFNB2	ephrin B2	No results	ACVRL1	activin A receptor like type 1	No results
ATF4	activating transcription factor 4	Apoptosis	SOX9	SRY-box transcription factor 9	Prognosis
IL1R1	interleukin 1 receptor type 1	No results	ARHGAP22	Rho GTPase activating protein 22	No results
FRMD6	FERM domain containing 6	Metastasis	PDGFC	platelet derived growth factor C	Angiogenesis
PSAP	Prosaposin	Proliferation	TNC	tenascin C	Metastasis
ITGA2	integrin subunit alpha 2	Progression	NRP2	neuropilin 2	Prognosis
PCSK5	proprotein convertase subtilisin/kexin type 5	No results	TLE3	TLE family member 3	No results
RHOJ	ras homolog family member J	No results	MYLK	myosin light chain kinase	Metastasis
ITGB5	integrin subunit beta 5	Migration	ABL2	ABL proto-oncogene 2	Prognosis
CD59	CD59 molecule	Hepatocarcinogenesis	COL1A2	collagen type I alpha 2 chain	Metastasis
CSF1	colony stimulating factor 1	Metastasis	SMURF2	SMAD specific E3 ubiquitin protein ligase 2	No results
THY1	Thy-1 cell surface antigen	Prognosis	TJP1	tight junction protein 1	Prognosis

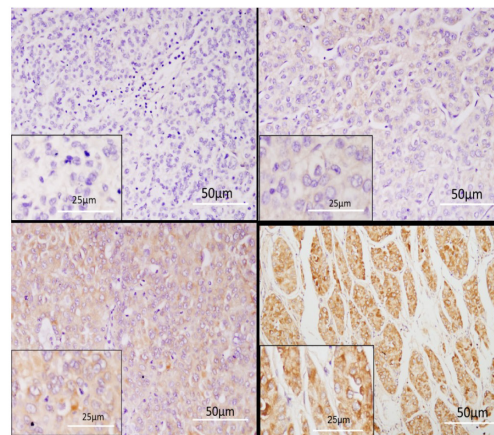
A



B



C



Supplementary Figure S1. A) The level of NRP1 mRNA and NRP1 protein in human L02 hepatocytes and several liver cancer cell lines (HepG2, Huh7, HCCLM3) were detected by qRT-PCR and western blot. Results are shown as means \pm SD. *p<0.05. **p<0.01. B) Nude mouse subcutaneous tumor tissue when transfected with HCCLM3-NC and HCCLM3-shNRP1 cells. C) The scoring standard of NRP1 expression after immunohistochemical staining.